Supplemental Information

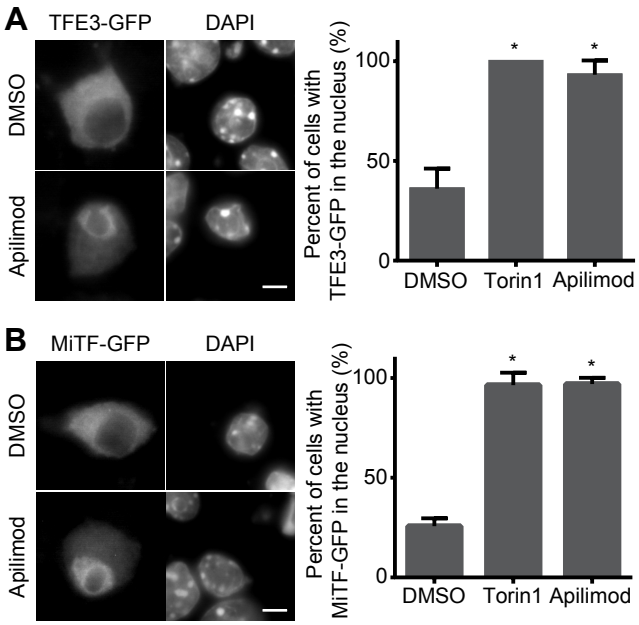

Supplemental Figure S1

Supplemental Figure S1: PIKfyve inhibition causes nuclear translocation of GFP-tagged TFE3 and MITF. RAW cells expressing TFE3-GFP (A) and MITF-GFP (B) treated with vehicle or apilimod as before. DAPI identifies the nuclei. Nuclear translocation was quantified by scoring the percent of cells with nuclear accumulation of these proteins. Shown is the mean percent and standard error of the mean from a minimum of 30 cells across at least three independent experiments. Asterisks (*) indicates statistical difference between conditions indicated by lines ($p<0.05$) using one-way ANOVA and Tukey's post-hoc test. Scale bar = 5 μm..

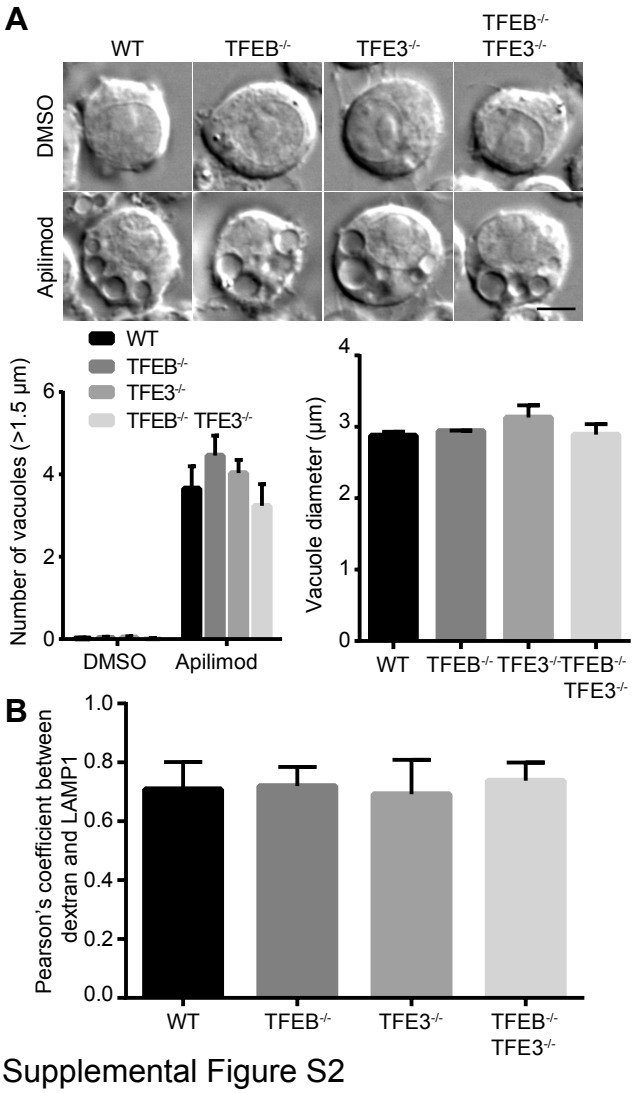

Supplemental Figure S2

Supplemental Figure S2: Manual quantification of vacuole diameter and number in wild-type, *tfeb*$^{-/-}$, *tfe3*$^{-/-}$ and *tfeb*$^{-/-}$ *tfe3*$^{-/-}$ double deleted cells inhibited for PIKfyve. A. Cells were incubated with vehicle or 20 nM apilimod for 1 h and then imaged by DIC optics. Mean vacuole number ± SEM and mean diameter ± SEM for vacuoles greater than 1.5 µm in diameter. B) Pearson's coefficient of dextran and LAMP1 in wild-type and RAW cells deleted for TFEB and/or TFE3. Data are from three independent experiments and from 100 cells or 300 vacuoles, respectively. No statistical difference was detected among apilimod-treated cell types.

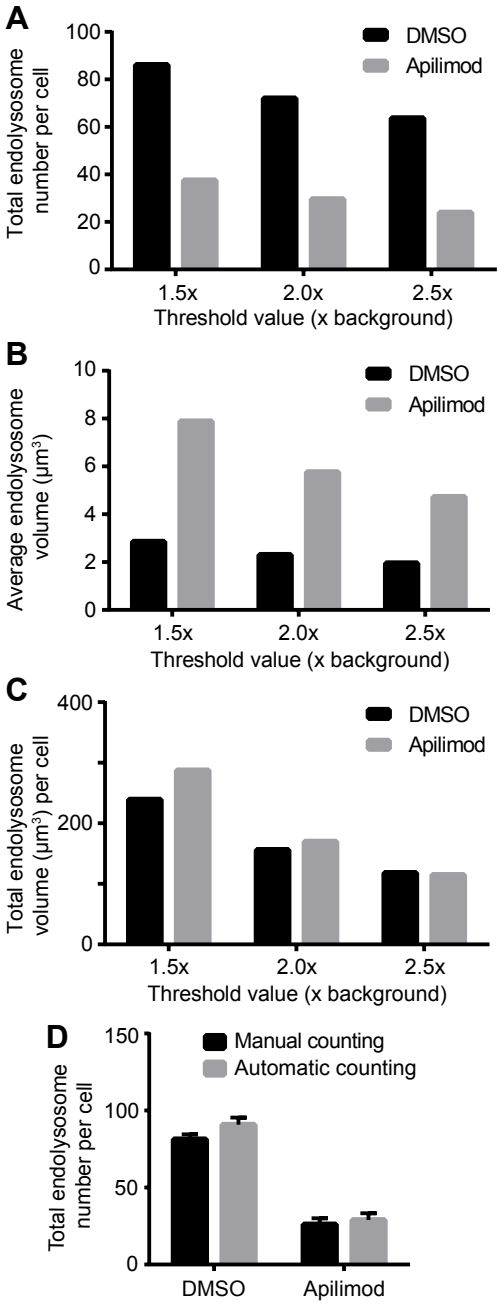

Supplemental Figure S3

Supplemental Figure S3: Comparison of endo/lysosome number, size and total endo/lysosome volume at different intensity thresholding values. Vehicle and apilimod-treated cells were imaged with the same parameters. A-C. Images were then subject to thresholding levels set at 1.5x, 2x and 2.5x that of cytosolic fluorescence intensity before volumetric analysis. Quantification of endo/lysosome number (A), endo/lysosome volume (B) and total endo/lysosome volume per cell (C). While the absolute values reduced with increasing thresholding, the relative trends between control and apilimod-treated cells remained similar across all thresholding measures. D. Number of endo/lysosomes counted manually and automatically at 2x thresholding and using a minimum particle size of 0.3 μm^3. In all cases, shown is the mean ± STD from 27 different cells.

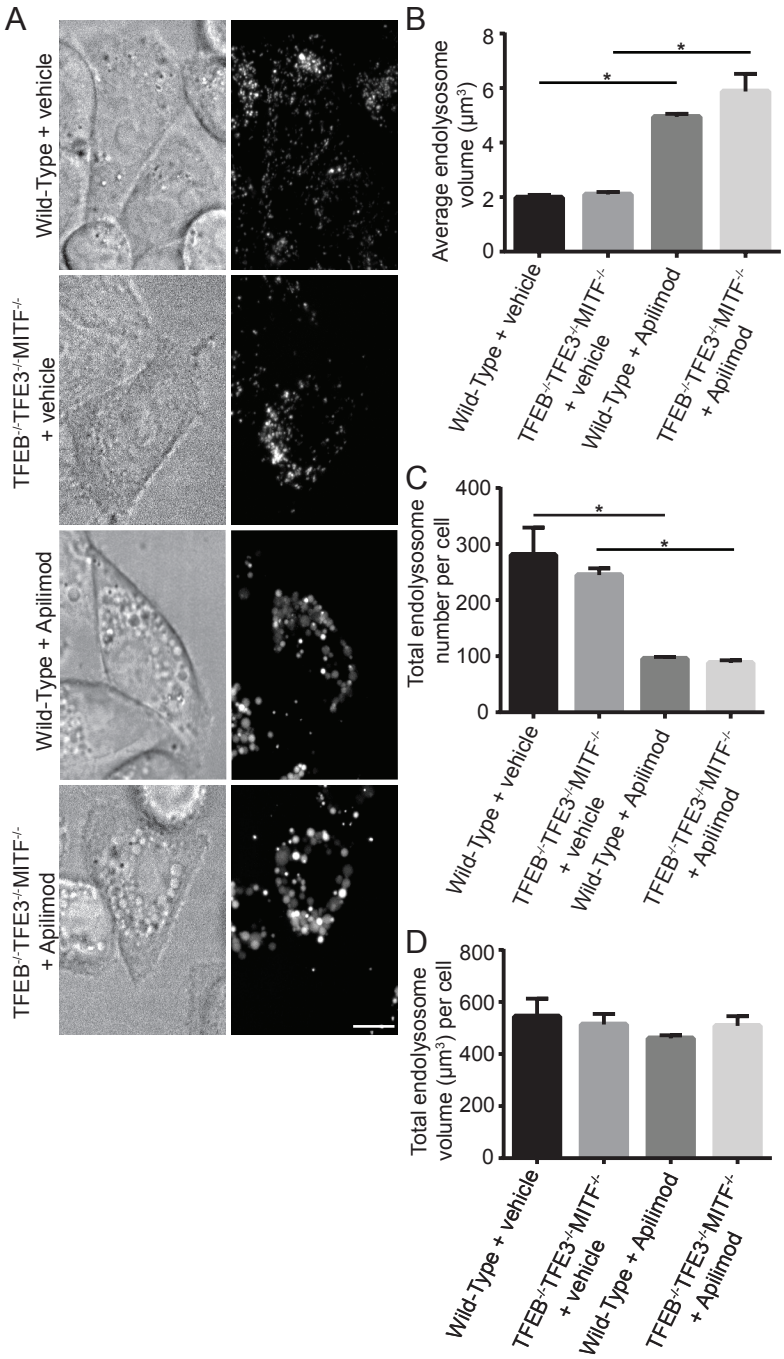

Supplemental Figure S4: Volumetric analysis of endo/lysosomes during acute PIKfyve suppression in HeLa cells. A. "Wild-type" HeLa cells and HeLa cells deleted for MITF, TFEB and TFE3 were pre-labelled with Alexa^{546}-conjugated dextran and treated with vehicle-only or 50 nM apilimod for 1 h. Quantification of endo/lysosome volume (B), number (C) and total endo/lysosome volume per cell (D). Shown is the mean ± SEM from 3 independent experiments and 15-20 cells per condition per experiment. Asterisk (*) indicates statistical difference relative to respective controls. No difference was observed between wild-type and mutant HeLa cells for changes during apilimod treatment. Scale bar = 10 µm.

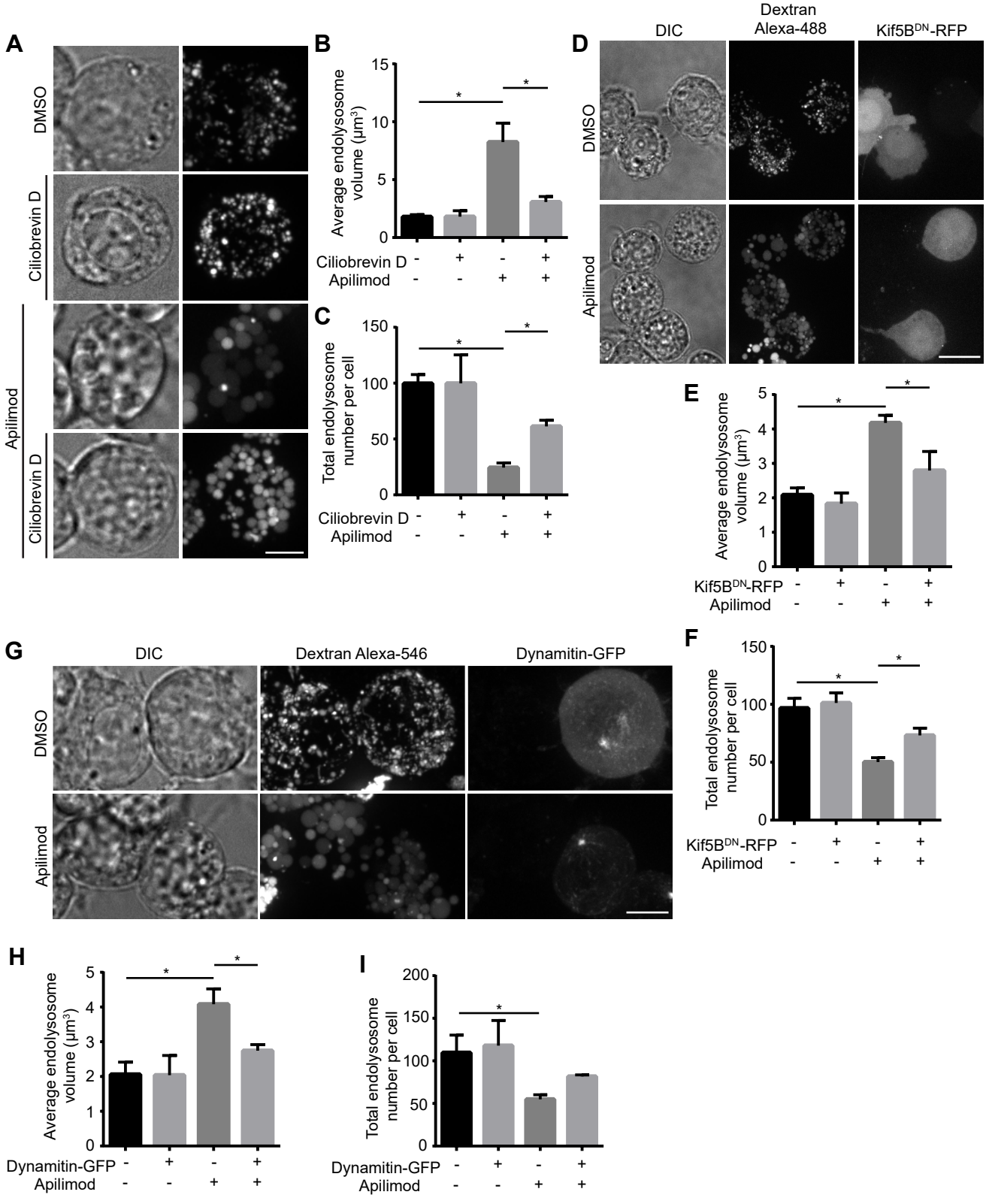

Supplemental Figure S5

Supplemental Figure S5: Volumetric analysis of endo/lysosomes during acute PIKfyve suppression in RAW cells disrupted for microtubule-motor proteins. A. Cells were pre-labelled with Alexa^{488}-conjugated dextran followed by DMSO alone or 1 h of 20 nM apilimod. This was then followed by vehicle or 100 µM ciliobrevin D for an additional 2.5 h in presence and absence of 20 nM apilimod 1 h. Scale bar = 5 µm. B, C. Volumetric quantification of endo/lysosome volume (B) and number (C) for *A*. D. Cells were transfected with dominant-negative kinesin (Kif5B^{DN}-RFP) to block kinesin. Cells were then pre-labelled with Alexa^{488}-conjugated dextran followed by vehicle-alone or apilimod 20 nM treatment for 30 min to induce vacuolation. Scale bar = 10 µm. E, F. Volumetric quantification of endo/lysosome volume (E) and number (F) for *D*. G. Cells were transfected with p50-dynamitin-GFP (Dynamitin-GFP) to block dynein. Cells were then pre-labelled with Alexa^{546}-conjugated dextran followed by vehicle-alone or apilimod 20 nM treatment for 30 min to induce vacuolation. Scale bar = 5 µm. H, I. Volumetric quantification of endo/lysosome volume (H) and number (I) for *G*. In all cases, data shown are the normalized mean ±SEM from three independent experiments, with at least 15-20 cells per condition per experiment. Asterisks (*) indicates statistical difference from respective control conditions.

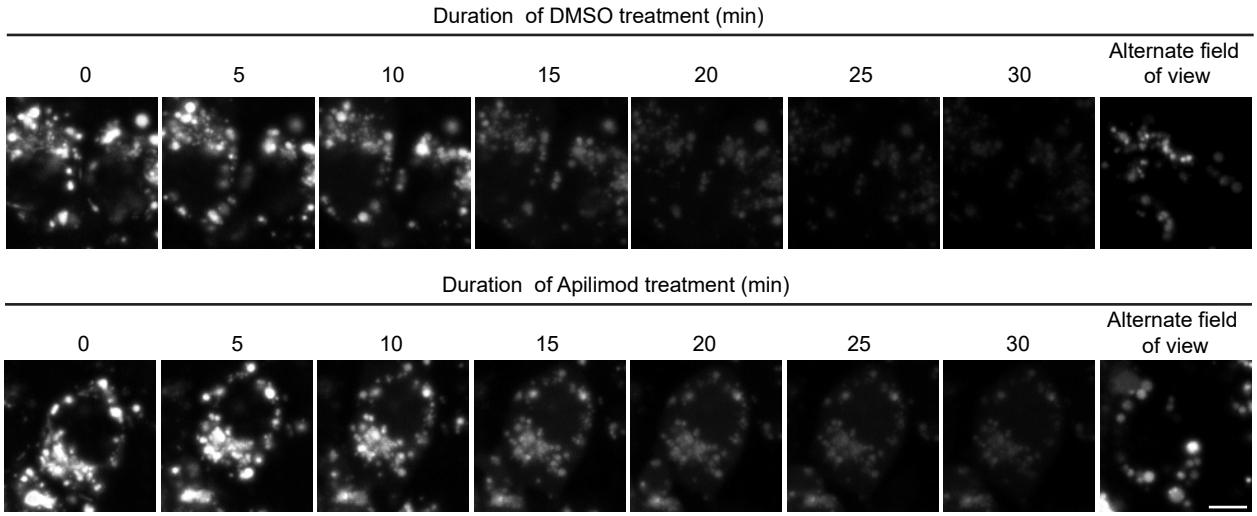

Supplemental Figure S6

Supplemental Figure S6: Live-cell imaging precludes lysosome enlargement. RAW macrophages were pre-labelled with Alexa^{546}-conjugated dextran as before. Cells were then imaged live by spinning disc confocal microscopy after the addition of vehicle or 20 nM apilimod every 10 s for 30 min with 6 z-slices imaged per time point. A. Time-sequence of vehicle-treated cells over 30 min. Frames are from Supplemental Movie 1. An alternate field of view from the same coverslip immediately post imaging shows lysosome signal at the end of 30 min of imaging. B. Time sequence of apilimod-treated cells showing no vacuolation over 30 min from Supplemental Movie 2. An alternate field of view from the same coverslip immediately post imaging shows lysosome enlargement elsewhere. Time shown in min. Scale bar = 5 µm.

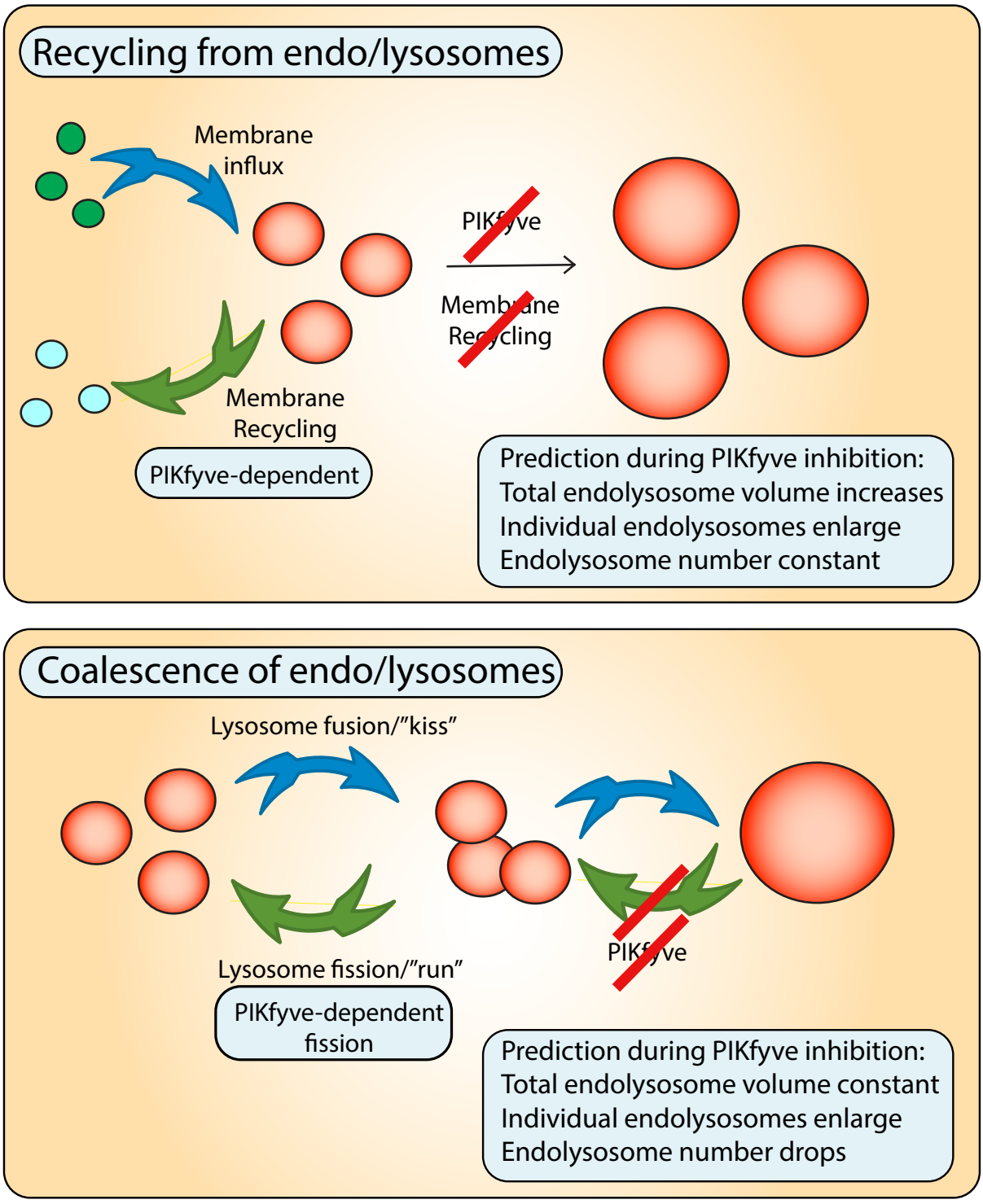

Supplemental Figure 7

Supplemental Figure S7: Models of endo/lysosome enlargement during PIKfyve inhibition. PIKfyve inhibition causes endo/lysosome enlargement. This may occur because of i) a defect in membrane recycling from endo/lysosomes and/or ii) due to endo/lysosome coalescence. A defect in membrane recycling should lead to an increase in total lysosome volume as membrane influx is no longer balanced by an efflux pathway. In this model, individual lysosomes should swell but their numbers remain similar. In comparison, endo/lysosomes undergo constant rounds of homotypic and heterotypic fusion and splitting. This may occur through full endo/lysosome merger, followed by splitting, or during partial fusion (kiss) and separation (run). Our work suggests that endo/lysosome enlargement proceeds through a failure to separate/run causing endo/lysosomes to become coalescence and enlarge. In this scenario, total lysosome volume should remain constant but the total numbers of endo/lysosomes should drop.

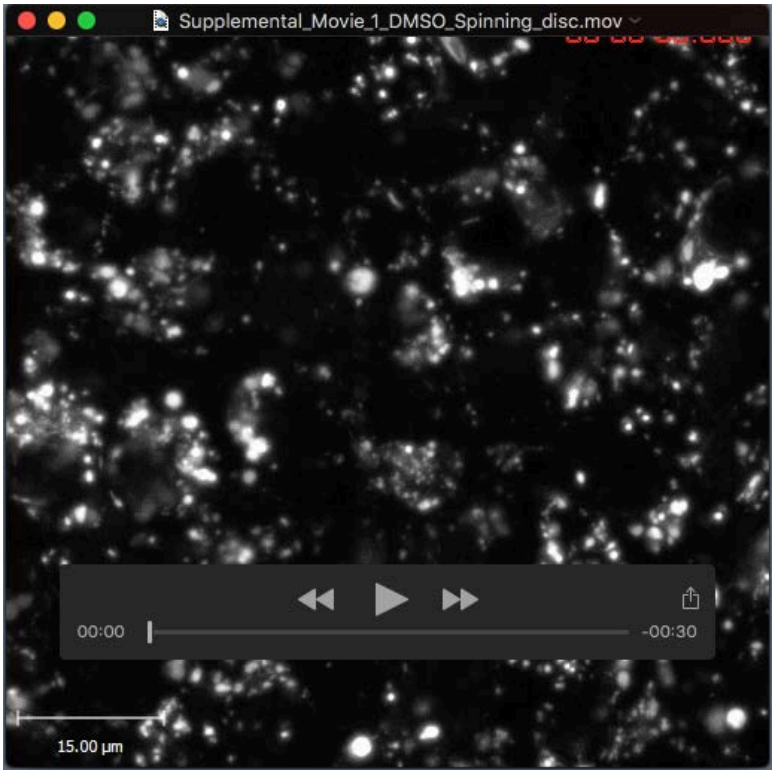

Supplemental Movie 1: Endo/lysosome dynamics of DMSO-treated cells at high-frame rate imaging using spinning disc confocal microscopy. RAW macrophages were pre-labelled with Alexa^{546}-conjugated dextran, followed by live-cell imaging using spinning disc confocal microscopy after the addition of DMSO. Imaging was done by acquiring 6 planes along the z-axis every 10 s for 30 min. Refer to Supplemental Figure S6 for select stills. Scale and time are indicated.

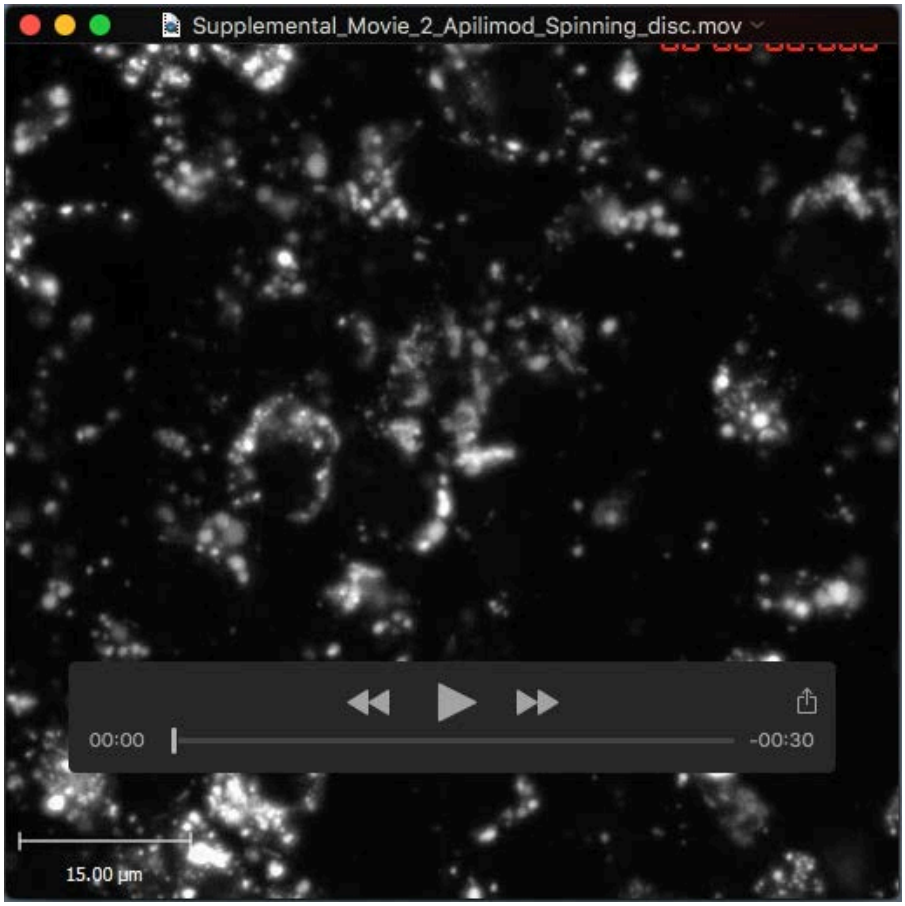

Supplemental Movie 2: Endo/lysosome dynamics of apilimod-treated cells at high-frame rate imaging using spinning disc confocal microscopy. RAW macrophages were pre-labelled with Alexa^{546}-conjugated dextran as before, followed by live-cell imaging using spinning disc confocal microscopy after the addition of 20 nM apilimod. Imaging was done by acquiring 6 planes along the z-axis once every 10 s for 30 min after apilimod addition. Refer to Supplemental Figure S6 for select stills. Vacuolation was not observed in the field under observation. Scale and time are indicated.

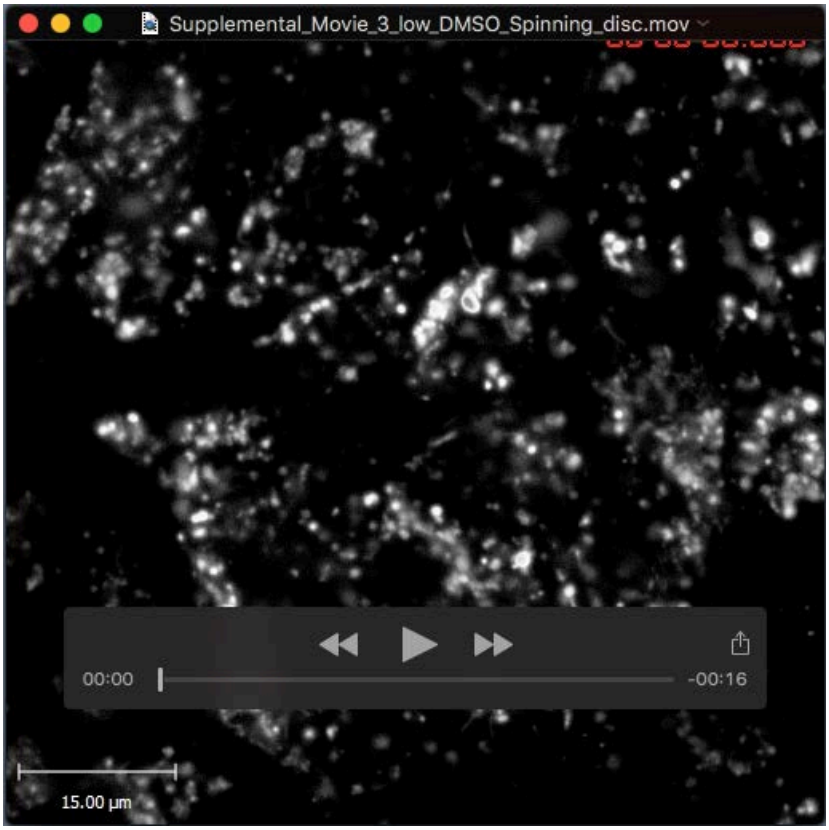

Supplemental Movie 3: Endo/lysosome dynamics of DMSO-treated cells at low-frame rate imaging using spinning disc confocal microscopy. RAW macrophages were pre-labelled with Alexa^{546}-conjugated dextran as before, followed by live-cell imaging using spinning disc confocal microscopy after the addition of DMSO. Imaging was done at a single-plane once every 2 min for 60 min. Refer to Figure 8A for select stills. Scale and time are indicated.

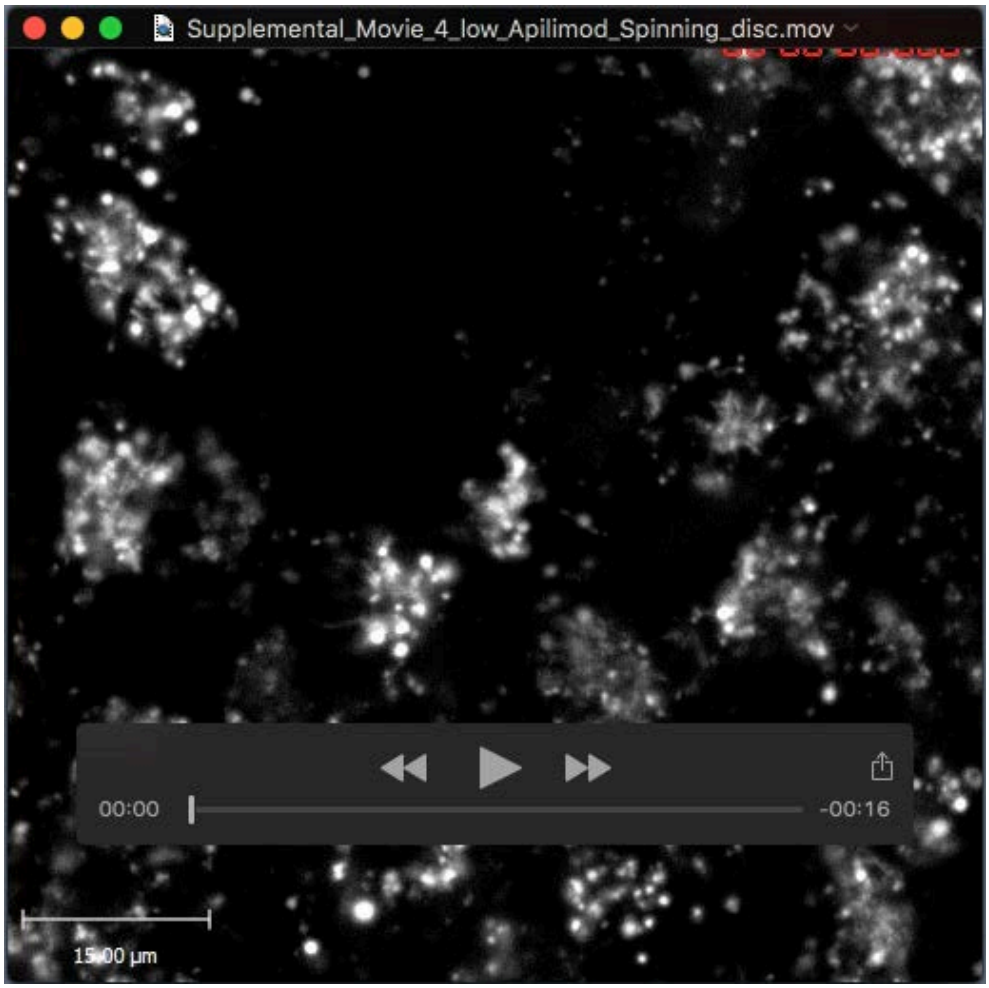

Supplemental Movie 4: Endo/lysosome dynamics of apilimod-treated cells at low-frame rate imaging using spinning disc confocal microscopy. RAW macrophages were pre-labelled with Alexa^{546}-conjugated dextran as before, followed by live-cell imaging using spinning disc confocal microscopy after the addition of 20 nM apilimod. Imaging was done at a single-plane once every 2 min for 60 min. Refer to Figure 8B for select stills. Vacuolation occurs during lower light exposure frequency. Scale and time are indicated.

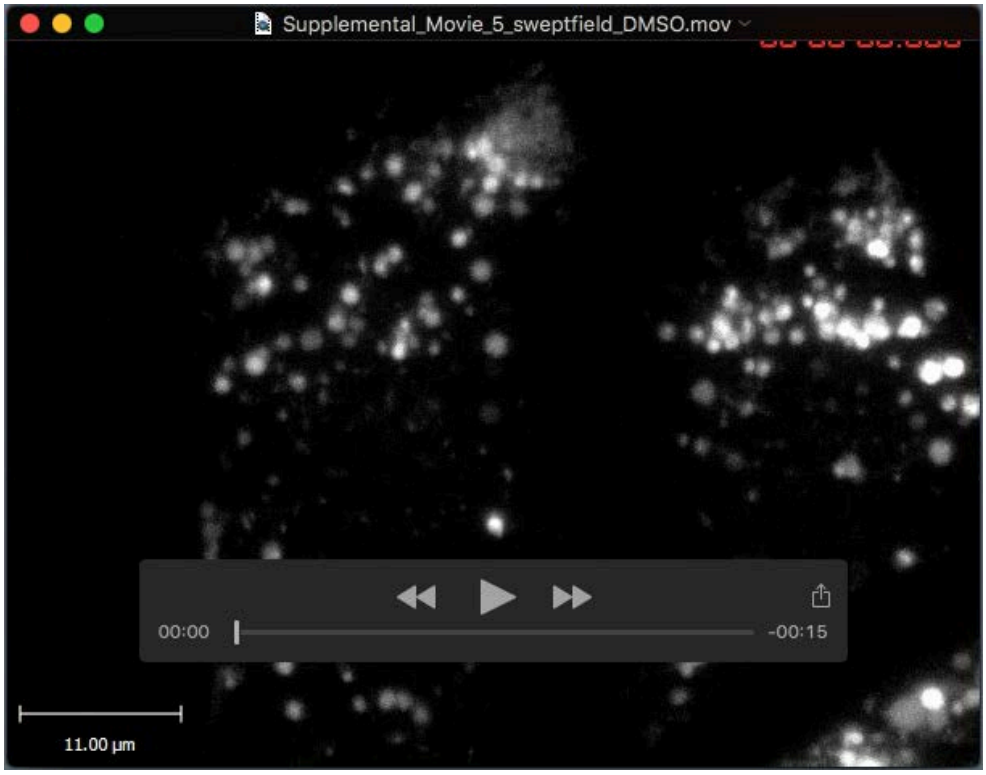

Supplemental Movie 5: Endo/lysosome dynamics of DMSO-treated cells at high-frame rate imaging using sweptfield confocal microscopy. RAW macrophages were pre-labelled with Alexa^{555}-conjugated dextran, followed by live-cell imaging using sweptfield confocal microscopy after the addition of DMSO. Imaging was done by acquiring 10 planes along the z-axis every 30 s for 30 min. The movie depicts a projection of all z-planes. Refer to Figure 8C for select stills. Scale and time are indicated.

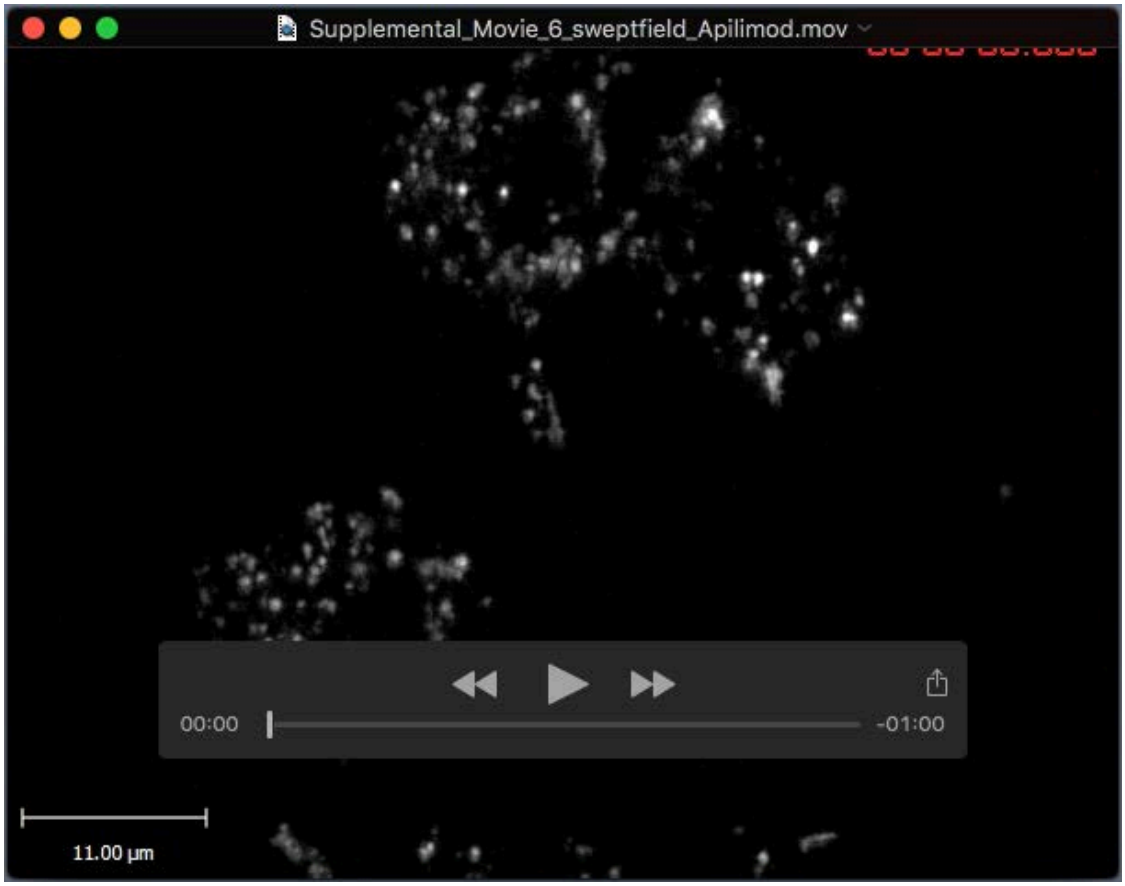

Supplemental Movie 6: Endo/lysosome dynamics of apilimod-treated cells at high-frame rate imaging using sweptfield confocal microscopy. RAW macrophages were pre-labelled with Alexa^{555}-conjugated dextran, followed by live-cell imaging using sweptfield confocal microscopy after the addition of 20 nM apilimod. Imaging was done by acquiring 10 planes along the z-axis every 30 s for 2 h. The movie depicts a projection of all z-planes. Refer to Figure 8D for select stills. Scale and time are indicated.